FOPID-Based Vacuum Control System Using a PWM-Regulated Buck Converter for neumatic Soft Actuation

Sistema de control de vacío basado en FOPID mediante un convertidor Buck regulado por PWM para actuación neumática suave

Valeria Arias Rocha[1], Horacio Rostro González[2,3], Felipe de J. Torres del Carmen[3], Leonardo Martínez Jiménez[4], Juan P. Ignacio Ramírez Paredes[3], Mario A. Juarez Balderas[1], Miroslava Cano Lara*[1]

[1]Tecnológico Nacional de México/ITESI
[2]Universidad Ramon Llull/School of Engineering, GEPI
[3]Universidad de Guanajuato/DICIS
[4]Universidad de Guanajuato/DEM

MIP25110001@irapuato.tecnm.mx
miroslava.cl@irapuato.tecnm.mx

Abstract

Soft neumatic actuators require accurate pressure regulation to achieve repeatable and stable deformation, particularly in vacuum-driven applications where the nonlinear behavior of the actuator and pneumatic system can affect the dynamic response. This work presents the development and experimental evaluation of a vacuum pressure control system for a soft neumatic actuator using a DC air pump driven through a Buck converter. The converter was controlled by a 20 kHz pulse-width modulation (PWM) signal, allowing the pump voltage and, consequently, the vacuum level applied to the actuator to be regulated. A pressure sensor was integrated into the system to provide feedback for closed-loop control. Two control strategies, a conventional proportional–integral–derivative (PID) controller and a fractional-order PID (FOPID) controller, were experimentally implemented and compared under different operating conditions. The results showed that the FOPID controller provided improved pressure tracking and reduced deviations from the reference signal compared with the conventional PID controller. The average tracking error was reduced from 15.70% with the PID controller to 1.78% with the FOPID controller. These results demonstrate that the proposed Buck-converter-based actuation system, combined with fractional-order control, provides an effective approach for improving vacuum regulation in soft pneumatic actuators and offers a suitable platform for future soft robotic applications requiring accurate and stable pressure control.

Keywords: Buck converter; pulse width modulation (PWM); FOPID controller; neumatic system; soft robotic actuators.

Introduction

Soft robotics has emerged as an alternative to conventional robotic systems due to its ability to adapt to variable geometries. Within this field, pneumatic actuators stand out for their low weight, flexibility, and ability to generate motion through variations in internal pressure. However, controlling them presents challenges related to the compressibility of air, leaks, and the system's nonlinear behavior (Oguntosin *et al*., 2017). To improve the performance of these actuators, one approach involves implementing electronic drive systems capable of precisely regulating internal pressure. In this context, Buck-type DC-DC converters controlled by pulse width modulation (PWM) allow the power supplied to a DC load to be adjusted by varying the duty cycle (Tavera Mosqueda *et al*., 2016), providing an alternative for electronically controlling DC pumps used in Neumatic systems. Neumatic pressure regulation is controlled using a FOPID (fractional-order proportional-integral-derivative) controller, which incorporates two additional parameters compared to a conventional PID and provides greater flexibility in adjusting the system's response (Al-Dhaifallah *et al*., 2018).

This paper proposes the design and implementation of a pneumatic vacuum control system based on a PWM-controlled Buck converter and an FOPID controller. The proposed architecture integrates a 12 V DC diaphragm vacuum pump, specified for a nominal vacuum condition of approximately −40 kPa, together with a power electronics stage to regulate its supply voltage and a pressure sensor to provide the feedback signal.

The FOPID controller adjusts the PWM duty cycle according to the pressure error. The objective is to develop a closed-loop system capable of regulating the vacuum pressure.

State of the Art

Pressure control in soft robotics pneumatic actuators has been addressed using various drive architectures and control strategies. Oguntosin *et al*. (2017) designed an electro-pneumatic platform based on fuzzy control and PWM modulation for soft actuators, integrating dual sources of positive and negative pressure. The system regulates pressures from 0 to 1.5 psi in positive mode and down to −5 psi in negative mode through the coordinated use of pumps and valves. Tavera Mosqueda *et al*. (2016) developed a PWM-regulated Buck-type CD-CD converter using Arduino, sizing the reactive components to control the power stage rather than acting directly on the load. Meanwhile, Bakeri *et al*. integrated an LM2596 step-down regulator into an Arduino Pro Mini-based platform for a rehabilitation actuator, demonstrating the feasibility of incorporating voltage-reduction stages.

Kalisky *et al*. (2017) developed a closed-loop differential pressure control system using a PID controller for 3D-printed fluidic actuators. Its architecture integrated positive pressure and vacuum, which increased the working range and clamping force by 54% compared to the exclusive use of negative pressure and by 43% compared to positive pressure alone. This approach demonstrates the advantages of dual systems for optimizing mechanical performance in soft robotics. Hanson *et al*. (2024) implemented a discrete closed-loop PID control system for a negative-pressure-driven Kresling-type origami actuator; they used capacitive sensors to compensate for its nonlinear behavior and achieved errors of less than 3 mm. To address the pneumatic complexity, fractional-order strategies were employed.

Al-Dhaifallah *et al*. (2018) proposed a FOPID controller with fuzzy tuning, which outperformed conventional PID and FOPID controllers in terms of response speed and disturbance rejection. Subsequently, Zhu *et al*. (2022) optimized an FOPID for pneumatic valves using an improved biogeographic algorithm (IBBO-FOPID), reporting an overshoot of only 0.676% and a settling time of 3.53 s, outperforming the Ziegler-Nichols method. Finally, He *et al*. (2025) refined this approach by combining genetic algorithms and Hippopotamus Optimization, achieving a settling time of 5.25 s and an overshoot of 0.88%, thereby consolidating the robustness of fractional-order strategies in pneumatic systems.

Methodology

This section presents the general system architecture, the design of the Buck converter, the generation of PWM signals, the operation of the vacuum pump, and the control strategy used for closed-loop pressure regulation.

General System Architecture

The proposed architecture is based on an electro-pneumatic negative-pressure control system consisting of a power electronics stage, a soft actuator, and a measurement system to implement a closed-loop control strategy. Similar pressure-control architectures have been reported in soft robotics, where sensor feedback is used to regulate positive and negative pressure inside soft actuators (Oguntosin *et al*., 2017). In particular, Oguntosin *et al*. demonstrated closed-loop regulation of negative pressure using a vacuum pump and pressure feedback in silicone-based soft robots. The system receives as input a user-set pressure reference, which is compared with the pressure measured inside the actuator by a pressure sensor. The difference between these two signals represents the control error, which is processed by the FOPID controller to generate a pulse-width modulation (PWM) signal. Fractional-order PID controllers have previously been applied to neumatic pressure regulation because their additional fractional parameters provide greater flexibility for controlling nonlinear pressure dynamics (Al-Dhaifallah *et al*., 2018; Massoud *et al*., 2025).

This architecture is based on the electro-pneumatic systems used in soft robotics, where pressure regulation requires the integration of sensors, actuators and control algorithms due to the nonlinear behavior associated with air compressibility and the mechanical characteristics of soft actuators. Oguntosin *et al* (2017) emphasize that a pneumatic control system must incorporate a pressure or vacuum source, actuators, sensors, and a control strategy capable of continuously correcting the actuator pressure.

Buck Converter Design

The Buck converter is used as a power conditioning stage between the power supply and the vacuum pump. Its primary function is to modulate the voltage applied to the motor using a PWM signal, allowing the rotational speed—and, therefore, the level of vacuum generated—to be regulated. The converter's operating on the controlled switching of a power semiconductor device, when the electronic switch remains on for a fraction of the switching period, the energy stored in the inductor increases; subsequently, during the off state, the stored energy is transferred to the load through the freewheeling diode. The relationship between the output voltage and the duty cycle is primarily determined by:

$$V_o = DV_{in} \qquad (1)$$

where V_o corresponds to the average output voltage, V_{in} is the input voltage, and D represents the duty cycle of the PWM signal. Young *et al*. (2021) employed a stage based on a buck converter to electrically control pumps and proportional valves within a pneumatic system, using a constant-frequency PWM signal with a variable duty cycle to modulate the voltage applied to the actuator.

The buck converter was sized to step down an input voltage of 15 V to a maximum of 12 V, corresponding to the nominal voltage pump operation. A switching frequency of 20 kHz was set, and, assuming a rated current of 0.5 A, an equivalent load of 24 Ω was obtained. The calculated nominal duty cycle was 80%, while the critical inductance was 120 µH, matching the inductor used in the experiment. A 470 µF output capacitor was also selected to reduce voltage ripple. The duty cycle is varied to regulate the pump's power supply, which begins operating at approximately 30%.

$$D = \frac{Vin}{Vo} = 0.80 \qquad (2)$$

Pump's equivalent resistance for $I_o = 0.5\,A$:

$$R = \frac{Vo}{Io} = 24\Omega \qquad (3)$$

The critical inductance:

$$L = \frac{(1-D)R}{2fs} = 120\mu H \qquad (4)$$

The inductor ripple current:

$$\Delta IL = \frac{(Vin-Vo)D}{Lfs} = 13.3mV \qquad (5)$$

Figure 1(a) shows the PSpice implementation of the PWM-controlled buck converter used to regulate the DC pump supply. The converter was designed with an input voltage of 15 V, a switching frequency of 20 kHz, an inductance of 120 µH, an output capacitor of 470 µF, and an equivalent load of 24 Ω. Figure 1(b) presents the transient output voltage response obtained from a parametric sweep of the duty cycle from 30% to 80%. As the duty cycle increases, the output voltage rises progressively. During startup, a transient response is observed due to the energy exchange between the inductor and capacitor; afterward, the signals approach steady-state operation. These results verify the expected behavior of the converter within the selected operating range for regulating the pump supply.

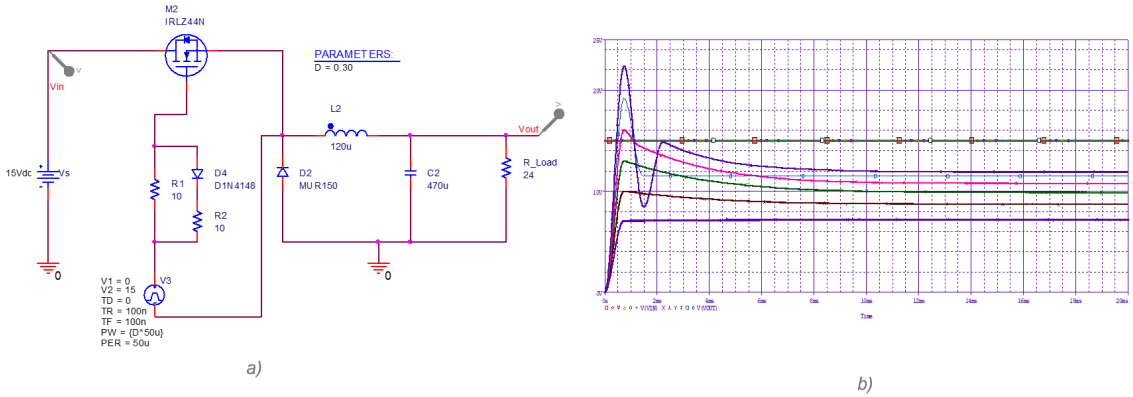


Figure 1. a) PSpice simulation schematic of the PWM-controlled buck converter for DC pump regulation. b) Transient output voltage response for duty cycles from 30% to 80% at 20 kHz.
Source: Author's own elaboration.

Figure 2 shows the physical implementation of the proposed vacuum pressure control system. Figure 2(a) presents the assembled prototype, including the electronic control stage, buck converter, pressure sensing components, and DC vacuum pump. Figure 2(b) shows the complete experimental setup used during validation, including the oscilloscope, multimeter, and computer for signal monitoring and data acquisition.

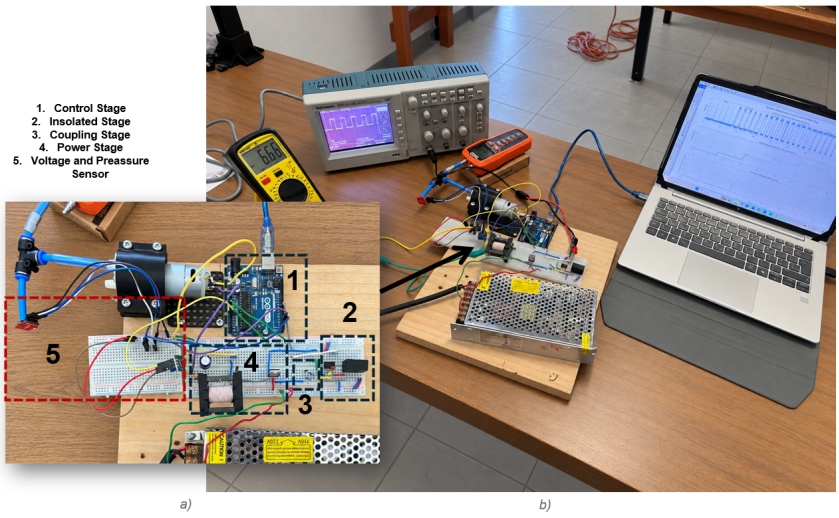


Figure 2. a) Assembled electronic and pneumatic prototype. b) Complete experimental setup with measurement and data acquisition equipment.
Source: Author's own elaboration.

MOSFET Isolation and Drive Stage

Figure 3 shows the electronic architecture used to interface the Arduino UNO with the buck converter power stage. The electronic schematic was developed using KiCad. The HCPL-3120 isolated controller was used to drive the MOSFET; it is responsible for adapting the 20 kHz PWM signal from the microcontroller to the levels required by the power stage. Its output was powered by an isolated 15 V power supply, enabling proper MOSFET drive and providing electrical isolation between the control and power stages. A 10 Ω gate resistor was also incorporated to limit the current during switching.

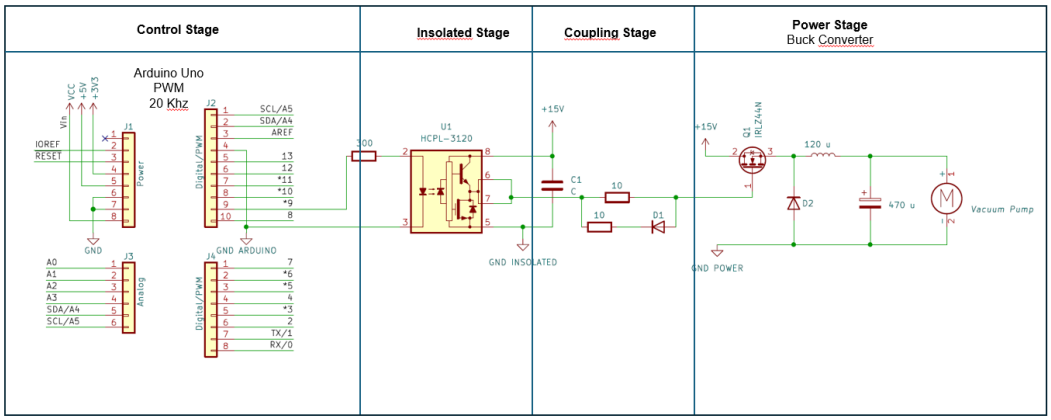


Figure 3. Electronic drive architecture comprising the control, isolation, gate-drive coupling, and buck converter power stages for DC vacuum pump regulation. Source: Author's own elaboration.

PWM Generation

The PWM signal was generated using an Arduino UNO microcontroller with a switching frequency of 20 kHz. To verify its operation, the PWM waveform was measured using an oscilloscope, and duty cycles of 0, 20, 40, 60, 80, and 100% were experimentally compared with their ideal signals, as shown in Figure 4. Subsequently, to control the pump using the buck converter, the duty cycle was used as the manipulated variable and was limited to the defined operating range of 30 to 80%.

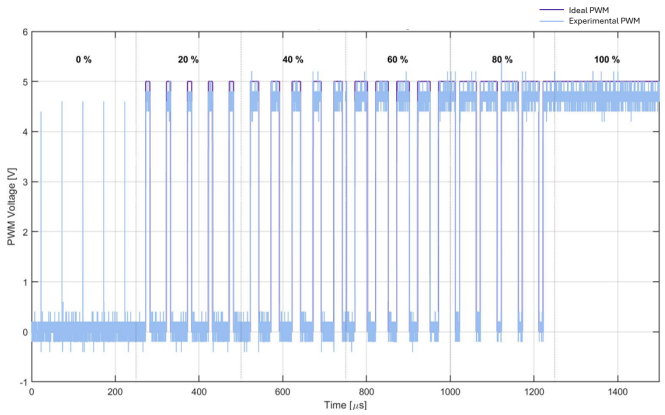


Figure 4. Ideal and experimental PWM signals comparison at 20 kHz for different duty cycles. Source: Author's own elaboration.

Neumatic Depressurization System

Neumatic systems used in soft robotics present challenges associated with air compressibility, leaks, and variations in actuator response. For this reason, various studies have incorporated pressure sensors as feedback elements to improve control accuracy. The neumatic system was implemented using a PYSP385-12V DC diaphragm pump, with a nominal voltage of 12 V, connected via a 6-mm polyurethane hose and neumatic connectors. The system pressure was measured using a sensor that served as a feedback element for the PID controller. The pump speed was regulated via the buck converter by varying the PWM duty cycle, allowing the system's depressurization level to be adjusted. The data sheet specifies a nominal voltage of 12 V and an operating range of 9.6 to 14.4 V. Neumatic systems used in soft robotics present challenges associated with air compressibility, leaks, and variations in actuator response. In this context, various studies have incorporated pressure sensors as feedback elements to improve control accuracy (Oguntosin *et al*., 2017).

FOPID Control Strategy

A fractional-order PID (FOPID) controller is implemented for pressure regulation; this controller represents an extension of the conventional PID controller through the incorporation of fractional orders in the integral and derivative terms (Al-Dhaifallah *et al*., 2018). The controller's primary function is to minimize the difference between the setpoint pressure and the measured pressure by generating a control signal that modifies the PWM duty cycle applied to the buck converter. The FOPID controller can be expressed as:

$$u(t) = K_p e(t) + K_i D^{-\lambda} e(t) + K_d D^{\mu} e(t) \qquad (6)$$

where K_p, K_iy K_d represent the proportional, integral, and derivative gains; while que λ and μ correspond to the fractional orders of integration and differentiation. Al-Dhaifallah *et al*. (2018) demonstrated that FOPID controllers can improve the response of neumatic systems due to the greater flexibility provided by the fractional parameters, thereby reducing response times and improving robustness against disturbances.

Closed-Loop Pressure Control System

The control algorithm was implemented on an Arduino UNO microcontroller with a sampling period of 100 ms. The signal acquired by the pressure sensor is processed using a five-sample median filter and a first-order 1-Hz low-pass filter to reduce spikes and measurement noise; subsequently, the error between the reference value and the measured vacuum level is calculated and processed by a FOPID controller with parameters $Kp = 6, Ki = 0.4,\ kd = 0.15,\ \lambda = 0.9,\ \mu = 0.8.$

The fractional-order integral and derivative operators were implemented using the Grünwald–Letnikov approximation with finite memory. The control action generated by the FOPID is combined with a PWM reference value obtained experimentally from open-loop tests, and finally, the resulting signal is limited to a range of 0 to 100% and applied to the Buck converter via a 20 kHz PWM signal to regulate the speed of the vacuum pump.

Results

Open-Loop Pressure System Characterization

Figure 5 presents the open-loop characterization of the pneumatic system for different PWM duty cycles. The experimental results show the relationship between the PWM command, the buck converter output voltage, and the vacuum pressure generated by the pump. No significant vacuum generation was observed at the lowest operating levels, whereas increasing the duty cycle produced a progressive increase in both the converter output voltage and the vacuum pressure. This behavior confirms that the PWM duty cycle can be used as the manipulated variable for pressure regulation.

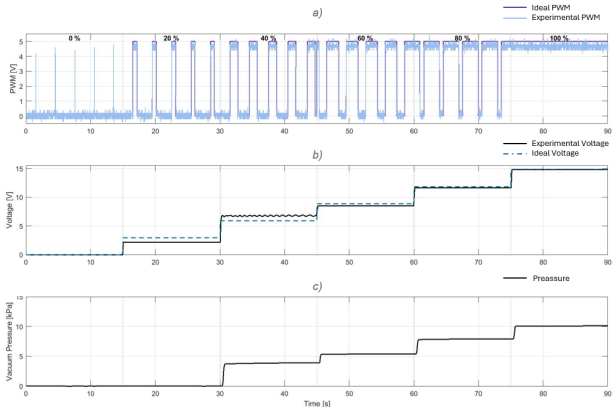


Figure 5. Open-loop characterization of the PWM-controlled buck converter and vacuum pressure response for different duty cycles. Source: Author's own elaboration. a) Experimental and Ideal PWM, b) Experimental and Ideal Voltage Output, c) Vacuum Pressure Magnitude.

This characterization is relevant for soft robotic applications because it establishes the relationship between the electrical command and the vacuum level applied to the actuator. By adjusting the PWM duty cycle, the pressure can be modified gradually, enabling smoother and more controlled actuation of the soft robotic system.

PID Controller Response

Figure 6 shows the closed-loop pressure response obtained with the PID controller at four operating points corresponding to 40, 60, 80, and 100% duty cycle conditions, with desired vacuum pressure references of 8.97, 11.35, 14.92, and 16.66 kPa, respectively. During the initial depressurization stage, the vacuum level increases progressively until approaching the desired reference. The system exhibits a stable response with small oscillations around the steady state. In Fig. 6(a), corresponding to the 40% duty cycle and a reference pressure of 8.97 kPa, the system tracks the desired value with a relatively small steady-state error. As the operating point increases, a larger deviation from the reference is observed, particularly in Fig. 6(c) and Fig. 6(d), corresponding to reference pressures of 14.92 and 16.66 kPa, respectively, where the achieved vacuum pressure remains below the desired value. Transient peaks are observed at some operating points due to the corrective action of the PID controller and the dynamic response of the vacuum pump during the depressurization process.

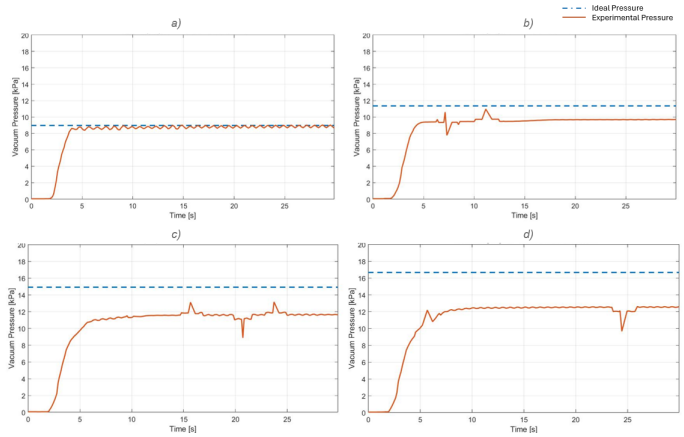


Figure 6. PID-controlled vacuum pressure response at four operating points: a) 40, b) 60, c) 80 and d) 100% duty-cycle. Source: Author's own elaboration.

FOPID Controller Response

Following the proposed methodology, Figure 7 shows the closed-loop pressure response obtained with the FOPID controller at four operating points corresponding to duty cycles of 40, 60, 80, and 100%. The FOPID controller achieved vacuum pressures of 9.36, 11.49, 15.13, and 16.66 kPa, respectively, for reference values of 8.97, 11.35, 14.92, and 16.66 kPa. At the higher operating points of 80 and 100%, the FOPID response approached the reference more effectively than the conventional PID controller, which reached only 11.63 and 12.55 kPa, respectively.

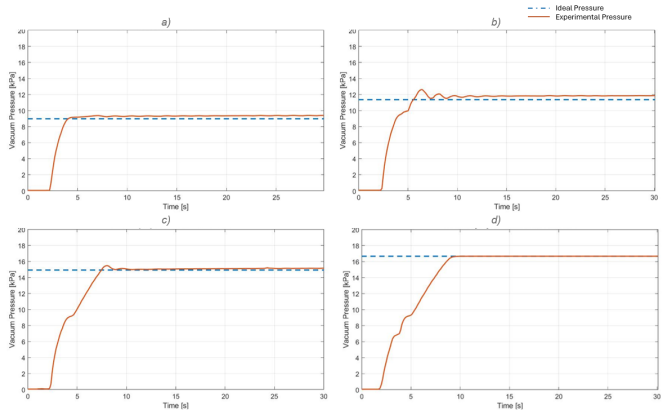


Figure 7. FOPID-controlled vacuum pressure response at four operating points: a) 40, b) 60, c) 80 and d) 100% duty-cycle. Source: Author's own elaboration.

PID vs. FOPID Comparison

Figure 8 presents a direct comparison between the PID and FOPID controllers at the four evaluated operating points. At 40% duty cycle, both controllers exhibit similar tracking performance, although the PID presents a slightly lower steady-state error. As the operating point increases, the advantage of the FOPID controller becomes more evident. At 60, 80, and 100%, the FOPID maintains the vacuum pressure closer to the desired reference, reducing the pressure loss observed with the conventional PID controller. Although small transient oscillations are observed during the settling process, particularly at intermediate operating points, the FOPID response converges more effectively to the reference. Therefore, the main improvement is not the complete elimination of pressure fluctuations, but a better regulation capability and lower steady-state pressure deviation, especially at higher duty-cycle conditions.

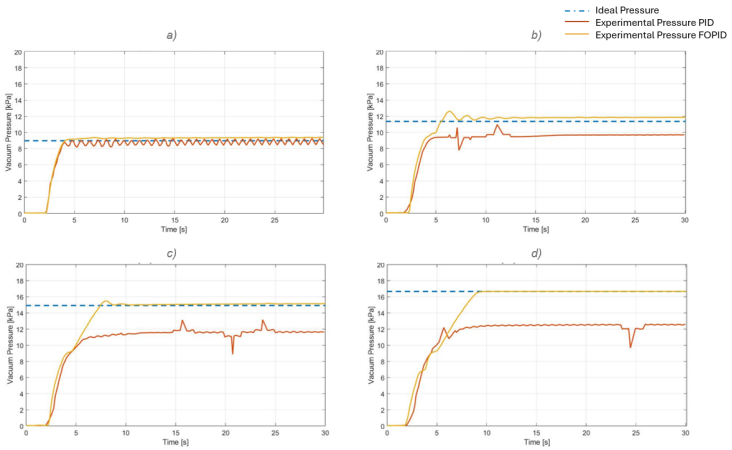


Figure 8. PID and FOPID comparison vacuum pressure responses at: a) 40, b) 60, c) 80 and d) 100% duty-cycle operating points. Source: Author's own elaboration.

FOPID Error Analysis

Figure 9 presents the distribution of the percentage error obtained with the FOPID controller at the four evaluated operating points. The errors remain below the established 5% tolerance limit in all cases. For duty cycles of 40 and 60%, the error is concentrated around 4.3–4.5%, while for 80% it decreases to approximately 1.5%. For a 100% duty cycle, the error approaches zero. These results indicate that the FOPID controller maintains the tracking error within the defined tolerance over the entire evaluated operating range.

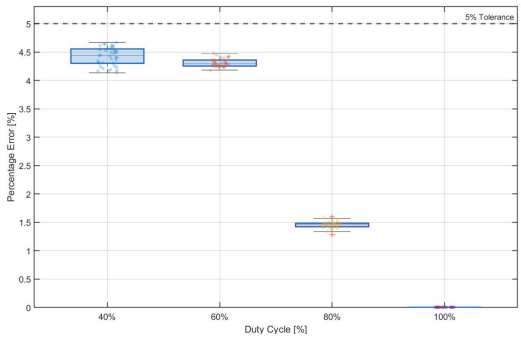


Figure 9. Percentage error distribution of the FOPID controller at 40, 60, 80, and 100% duty cycle, considering a 5% tolerance limit. Source: Author's own elaboration.

Table 1 summarizes the steady-state performance of the PID and FOPID controllers at the four operating points evaluated. The results show that, although the PID controller presents the lowest error at 40% duty cycle, the FOPID controller achieves considerably lower errors at 60, 80, and 100%, demonstrating improved reference tracking as the operating point increases.

***Table 1**. Comparison of steady-state vacuum pressure and percentage error for PID and FOPID controllers at different duty cycles.*

Duty Cycle [%]	Reference Pressure [kPa]	PID Pressure [kPa]	PID Error [%]	FOPID Pressure [kPa]	FOPID Error [kPa]
40	8.97	8.84	1.37	9.36	4.42
60	11.35	9.68	14.72	11.49	1.23
80	14.92	11.63	22.03	15.13	1.45
100	16.66	12.55	24.67	16.66	0.01

Conclusions

This work experimentally validated a PWM-regulated, buck-converter-driven DC pump architecture for high-precision vacuum pressure regulation in soft pneumatic systems. Open-loop characterization mapped the steady-state pressure response, achieving discrete vacuum levels of 8.97, 11.35, 14.92, and 16.66 kPa across 40, 6, 80 and 100 duty cycles, respectively. Under closed-loop operation, the fractional-order PID (FOPID) controller significantly outperformed the conventional PID framework, reducing the average steady-state error from 15.70% to 2.55% representing an 83.8% error reduction, while delivering superior reference tracking at higher operating points. These findings confirm that the proposed FOPID and power-electronic integration provides a robust, high-fidelity actuation platform for advanced soft robotic applications requiring stringent dynamic pressure control.

Acknowledgment

This work was supported by the project SIRA-PVR-2026-25454 of National Technological Institute of Mexico. The authors also acknowledge the Secretaría de Ciencia, Humanidades, Tecnología e Innovación (SECIHTI) and the Master's Program in Electronics for their support in the development of this research.

References

Al-Dhaifallah, M., Kanagaraj, N., & Nisar, K. S. (2018). Fuzzy fractional-order PID controller for fractional model of pneumatic pressure system. *Mathematical Problems in Engineering, 2018*, Article ID 5478781.

Bakeri, H., Hasikin, K., Abd Razak, N. A., Mohd Razman, R., Khamis, A. A., Annuha, M. 'A., Tajuddin, A., & Reza, D. (2023). Silicone elastomeric-based materials of soft pneumatic actuator for lower-limb rehabilitation: Finite element modelling and prototype experimental validation. *Applied Sciences, 13*(5), Article 2977.

Hanson, N., Mensah, I. A., Roberts, S. F., Healey, J., Wu, C., & Dorsey, K. L. (2024). Controlling the fold: Proprioceptive feedback in a soft origami robot. *Frontiers in Robotics and AI, 11*, Article 1396082.

He, Y., Ma, A., Wang, Y., Tian, X., & Zhao, S. (2025). FOPID controller design for pneumatic control valves with ultra-low overshoot, rapid response and enhanced robustness. *Scientific Reports, 15*, Article 4541.

Kalisky, T., Wang, Y., Shih, B., Drotman, D., Jadhav, S., Aronoff-Spencer, E., & Tolley, M. T. (2017). Differential pressure control of 3D printed soft fluidic actuators. In *2017 IEEE/RSJ International Conference on Intelligent Robots and Systems (IROS)* (pp. 6207–6213). IEEE.

Massoud, M. M., Alves, P. H. T. F., & Libby, J. (2025). Enhancing dual-loop pressure control in pneumatic soft robotics with a comparison of evolutionary algorithms for PID & FOPID controller tuning. *IEEE Robotics and Automation Letters, 10*(6), 6119–6126.

Oguntosin, V., Nasuto, S. J., & Hayashi, Y. (2017). Embedded fuzzy logic controller for positive and negative pressure control in pneumatic soft robots. In *2017 UKSim-AMSS 19th International Conference on Modelling & Simulation* (pp. 63–68). IEEE.

Tavera Mosqueda, S., Pérez Romero, P., Silva Ortigoza, R., García Sánchez, J. R., Alba Juárez, J. N., & Hernández Márquez, E. (2016). Control del voltaje de salida de un convertidor buck por medio de PWM generado con Arduino. *Boletín UPIITA, 11*(56), 1–6.

Wang, Y., Wang, Y., Mushtaq, R. T., & Wei, Q. (2024). Advancements in soft robotics: A comprehensive review on actuation methods, materials, and applications. *Polymers, 16*(8), Article 1087.

Young, T. R., Xavier, M. S., Yong, Y. K., & Fleming, A. J. (2021). A control and drive system for pneumatic soft robots: PneuSoRD. In *2021 IEEE/RSJ International Conference on Intelligent Robots and Intelligent Systems (IROS)* (pp. 2822–2828). IEEE. https://doi.org/10.1109/IROS51168.2021.9635874

Zhu, M., Xu, Z., Zang, Z., & Dong, X. (2022). Design of FOPID controller for pneumatic control valve based on improved BBO algorithm. *Sensors, 22*(17), Article 6706. https://doi.org/10.3390/s22176706